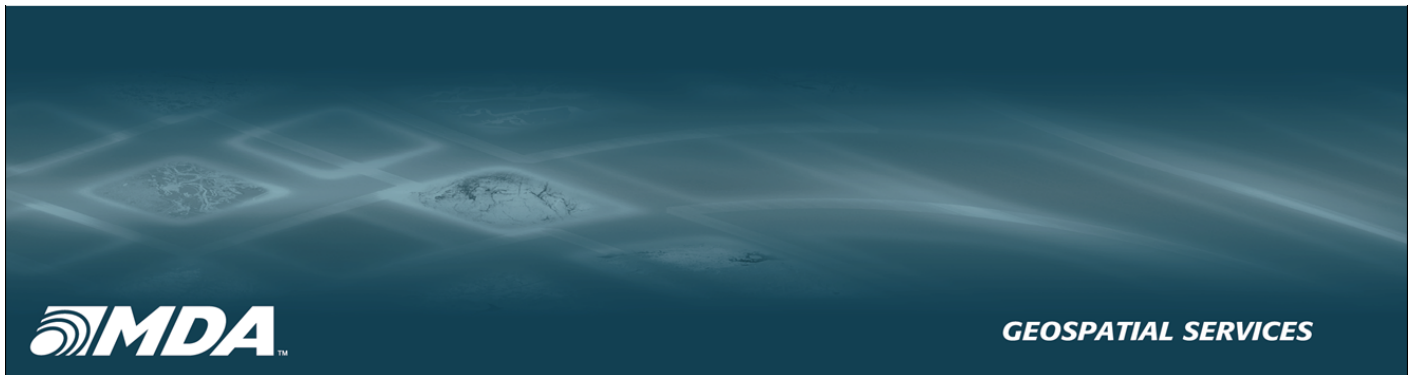


# Playa del Rey, California InSAR Ground Deformation Monitoring Interim Report E

Ref.: RV-14524  
July 20, 2011



SUBMITTED TO:

**Southern California Gas Company**  
555 W. Fifth Street (Mail Location 23E2)  
Los Angeles, CA, USA  
90013-1041

ATTN: Mr. Rick Gailing

SUBMITTED BY:

**MDA Geospatial Services**  
57 Auriga Drive, Suite 201  
Ottawa, Ontario K2E 8B2  
CANADA

Tel: +1-613-727-1087  
Fax: +1-613-727-5853

©MDA Geospatial Services Inc., 2011

All Rights Reserved

## **RESTRICTION ON USE, PUBLICATION OR DISCLOSURE OF PROPRIETARY INFORMATION**

This document contains information proprietary to MDA Geospatial Services Inc. ("MDA GSI"), its parent company MacDONALD, DETTWILER AND ASSOCIATES LTD., its subsidiaries or to a third party to which MDA GSI may have a legal obligation to protect such information from unauthorized disclosure, transfer, export, use or duplication. Any disclosure, use or duplication of this document or of any of the information contained herein for other than the specific purposes for which it was disclosed is expressly prohibited, except as MDA GSI may have otherwise agreed to in writing.





Prepared By: \_\_\_\_\_ July 20, 2011  
Mary Anne McParland  
Remote Sensing Analyst

Reviewed By: \_\_\_\_\_ July 20, 2011  
Shinya Sato  
Sr. Remote Sensing Analyst

Reviewed By: \_\_\_\_\_ July 20, 2011  
Gillian Robert  
Sr. Project Manager







## Executive Summary

This report, Interim Report E, describes the results and methodology used to monitor as well as quantify potential ground deformation at the Southern California Gas Company (SoCalGas) Playa del Rey Gas Storage Field and surrounding areas in Los Angeles using interferometric synthetic aperture radar (InSAR) satellite for the December 2010 to June 2011 monitoring time period.

The RADARSAT-2 satellite passes over SoCalGas' area of interest (AOI) every 24 days at an elevation of approximately 500 miles. The acquired RADARSAT-2 imagery is being used for the generation of deformation maps over the AOI, two of which are delivered to Southern California Gas Company (SoCalGas) every 6 months. The accuracy of each deformation map is estimated to be in the order of 0.02 ft.

The following summarizes key features for this deliverable:

- RADARSAT-2 Ultra-fine ascending satellite radar data were scheduled, acquired and analyzed from December 2010 through to June 2011.
- The highest quality deformation maps are generated. The time periods are from December 19, 2010 to March 1, 2011 (Pair A) and March 1, 2011 to June 29, 2011 (Pair B).
- The delivered products are geo-referenced with a horizontal accuracy better than 65 ft. Areas of insufficient quality are masked out in the final products. The measurements in the AOI are of good quality.
- The estimated precision for the pair December 19, 2010 to March 1, 2011 vertical deformation product is 0.02 ft with a 95% confidence interval; while the estimated precision for pair March 1, 2011 to June 29, 2011 vertical change product is 0.018 ft with a 95% confidence interval.
- For the latest time period analyzed, December 2010 to June 2011, large variations in precipitation have been recorded by the National Weather Service (Table 5). The variation in the reported InSAR ground surface movement is likely related to soil moisture changes. The majority of this variance is within the reported measurement of 0.02 ft, the noise level.





## Contents

<b>1 Interim Report E Objective</b>	<b>1</b>
1.1 Report Organization . . . . .	1
1.2 Study Area . . . . .	1
1.3 Data Selection . . . . .	3
<b>2 Results - Interim Report E</b>	<b>4</b>
2.1 Pair A - December 19, 2010 to March 1, 2011 . . . . .	5
2.2 Pair B - March 1, 2011 to June 29, 2011 . . . . .	10
2.3 Pair C - Cumulative Vertical Deformation December 19, 2010 to June 29, 2011 . . . . .	14
2.4 Pair D - Cumulative Vertical Deformation May 27, 2008 to June 29, 2011 . . . . .	17
<b>3 Concluding Remarks</b>	<b>20</b>
<b>A Deliverables</b>	<b>21</b>
<b>B Standard Definitions</b>	<b>22</b>



## List of Figures

1	Playa del Rey AOI and surrounding area in Los Angeles, as outlined by red polygon (radar amplitude image). . . . .	2
2	Playa del Rey Gas Storage Field AOI and surrounding area. Color representation of the vertical deformation product from December 19, 2010 to March 1, 2011 superimposed on SAR image without contours.	7
3	Playa del Rey Gas Storage Field AOI and surrounding area. Color representation of the vertical deformation product from December 19, 2010 to March 1, 2011 superimposed on SAR image with 0.01 ft contours. . . . .	8
4	Zoom-in of Playa del Rey Gas Storage Field AOI. Colour representation of the vertical deformation product from December 19, 2010 to March 1, 2011 superimposed on SAR image with 0.01 ft contours. . .	9
5	Playa del Rey Gas Storage Field AOI and surrounding area. Color representation of the vertical deformation product from March 1, 2011 to June 29, 2011 superimposed on SAR image without contours. . .	11
6	Playa del Rey Gas Storage Field AOI and surrounding area. Color representation of the vertical deformation product from March 1, 2011 to June 29, 2011 superimposed on SAR image with 0.01 ft contours.	12
7	Zoom-in of Playa del Rey Gas Storage Field. Cumulative vertical deformation from March 1, 2011 to June 29, 2011, with 0.01 ft contours.	13
8	Playa del Rey Gas Storage Field AOI and surrounding area. Color representation of the cumulative vertical deformation from December 19, 2010 to June 29, 2011 superimposed onto SAR image. . . . .	15
9	Zoom-in of Playa del Rey Gas Storage Field. Color representation of the summation of the vertical deformation products from December 19, 2010 to June 29, 2011 superimposed on SAR image with 0.01 ft contours. . . . .	16
10	Playa del Rey Gas Storage Field AOI and surrounding area. Color representation of the cumulative vertical deformation from May 27, 2008 to June 29, 2011 superimposed onto SAR image. . . . .	18
11	Zoom-in of Playa del Rey Gas Storage Field. Cumulative vertical deformation from May 27, 2008 to June 29, 2011, with 0.01 ft contours.	19
12	Definition of a 5.6-cm wave. . . . .	23
13	Electromagnetic spectrum. . . . .	24



## List of Tables

1	RADARSAT-2 Ultra-Fine data acquired over Playa del Rey Gas Storage Field . . . . .	3
2	Selected RADARSAT-2 data for the InSAR analysis . . . . .	3
3	Summary for Pair A . . . . .	4
4	Summary for Pair B . . . . .	4
5	Rainfall accumulation per month at LAX. Source: National Weather Service. . . . .	6
6	Delivered Data . . . . .	21



## List of Acronyms

**AOI** area of interest

**InSAR** interferometric synthetic aperture radar

**LAX** Los Angeles Airport

**SoCalGas** Southern California Gas Company

## 1 Interim Report E Objective

The objective of this report, Interim Report E, is to provide SoCalGas with measurements of the deformation that occurred within the project's area of interest (AOI) using conventional interferometric synthetic aperture radar (InSAR) monitoring from December 2010 to June 2011. For this Milestone, two conventional InSAR deformation maps quantifying movement were generated.

This deliverable pertains to the sixth deliverable, Milestone 6, of a five year InSAR Monitoring Program, as described in Section 2.1 Table 1 Milestone Deliverables of the Master Document.

### 1.1 Report Organization

This report is organized as follows:

- Section 1 provides the introduction and report organization. This section also describes the AOI and the available data for the current monitoring time period.
- Section 2 describes the results for the deformation maps as well as the cumulative vertical deformation products.
- Section 3 provides a summary and conclusions.
- Appendix A lists the deliverables.
- Appendix B provides a list of definitions for commonly used terms.

### 1.2 Study Area

The Playa del Rey Gas Storage Field AOI and surrounding area, in Los Angeles, California, is outlined by the red polygon, as seen in Figure 1. The corner coordinates for the polygon are approximately given by a rectangle with coordinates 34°01' 58"N 118°28' 5"W and 33°56' 56"N 118°20' 4"W.



Figure 1: Playa del Rey AOI and surrounding area in Los Angeles, as outlined by red polygon (radar amplitude image).



### 1.3 Data Selection

The RADARSAT-2 Ultra-Fine data used to generate the deliverables for the December 2010 to June 2011 time period are listed in Table 1 below.

Table 1: RADARSAT-2 Ultra-Fine data acquired over Playa del Rey Gas Storage Field

Acquisition #	Acquisition Date
1	December 19, 2010
2	January 12, 2011
3	February 5, 2011
4	March 1, 2011
5	March 25, 2011
6	April 18, 2011
7	May 12, 2011
8	June 5, 2011
9	June 29, 2011

The InSAR deformation maps created are listed in Table 2. On these dates, the SAR data were of best quality with suitable baselines. These two maps are generated using the March 1, 2011 acquisition as the shared data, which allows for a comparison between them.

Table 2: Selected RADARSAT-2 data for the InSAR analysis. The pairing numbers refer to the acquisition numbers from Table 1.

Interferogram Pair	Acquisition Date Master	Acquisition Date Slave	Perpendicular Baseline (meters)
A (1-4)	Dec-19-10	Mar-1-11	-13
B (4-9)	Mar-1-11	Jun-29-11	78



## 2 Results - Interim Report E

An analysis of the available data is carried out by evaluating all possible interferometric combinations. Two InSAR pairs are selected for the generation of deformation products:

- Pair A for the time period between December 19, 2010 to March 1, 2011 (72 days)
- Pair B for the time period between March 1, 2011 to June 29, 2011 (120 days)

These data are selected because the generated interferograms are of the best quality at these dates and are least affected by noise and the DEM error. A mask is applied to the incoherent areas. The root-mean-square of the observed values in the deformation map is indicative of the precision of the deformation map. To obtain a 95% confidence interval a factor of two is used. Table 3 and Table 4 show the summary of the estimation of noise level for Pairs A and B, respectively.

Table 3: Summary for Pair A

<b>Date</b>	<b>Time Span</b>	<b>Noise Level standard deviation [ft]</b>	<b>95% Confidence interval [ft]</b>
Dec-19-10 to Mar-1-11	72 days	0.01	0.02

Table 4: Summary for Pair B

<b>Date</b>	<b>Time Span</b>	<b>Noise Level standard deviation [ft]</b>	<b>95% Confidence interval [ft]</b>
Mar-1-11 to Jun-29-11	120 days	0.009	0.018

The following sections present the results for both pairs A and B.



## **2.1 Pair A - December 19, 2010 to March 1, 2011**

The vertical deformation in the Playa del Rey Gas Storage Field is observed for the time period between December 2010 to March 2011.

Deformation is observed in the AOI, as is shown from the vertical deformation product in Figure 2. In the south easterly limits of the Playa del Rey Storage Field Reservoir Boundary, (center co-ordinate 33°58'5"N 118°26'4"W) deformation values range from 0.03 to 0.04 ft uplift, as seen in Figure 4.

Uplift is seen in the Playa del Rey Gas Storage field from December 2010 to March 2011 and likely related to the higher amount of rainfall accumulated between those dates, as recorded by the National Weather Service at Los Angeles Airport (LAX) (Table 5).

A color representation of the vertical deformation product are shown in Figure 3 and Figure 4 after masking areas that contain noise. The estimated precision for Pair A is within  $\pm 0.02$  ft with a 95% confidence interval.



Table 5: Rainfall accumulation per month at LAX. Source: National Weather Service.

<b>Month</b>	<b>Monthly Precipitation [inches]</b>
June 2009	0.15
July 2009	0.00
August 2009	0.00
September 2009	Trace
October 2009	1.31
November 2009	0.00
December 2009	2.05
January 2010	6.01
February 2010	4.55
March 2010	0.21
April 2010	1.25
May 2010	0.00
June 2010	0.00
July 2010	Trace
August 2010	0.00
September 2010	Trace
October 2010	1.56
November 2010	0.59
December 2010	8.83
January 2011	0.81
February 2011	1.47
March 2011	4.04
April 2011	Trace
May 2011	0.53
June 2011	0.02

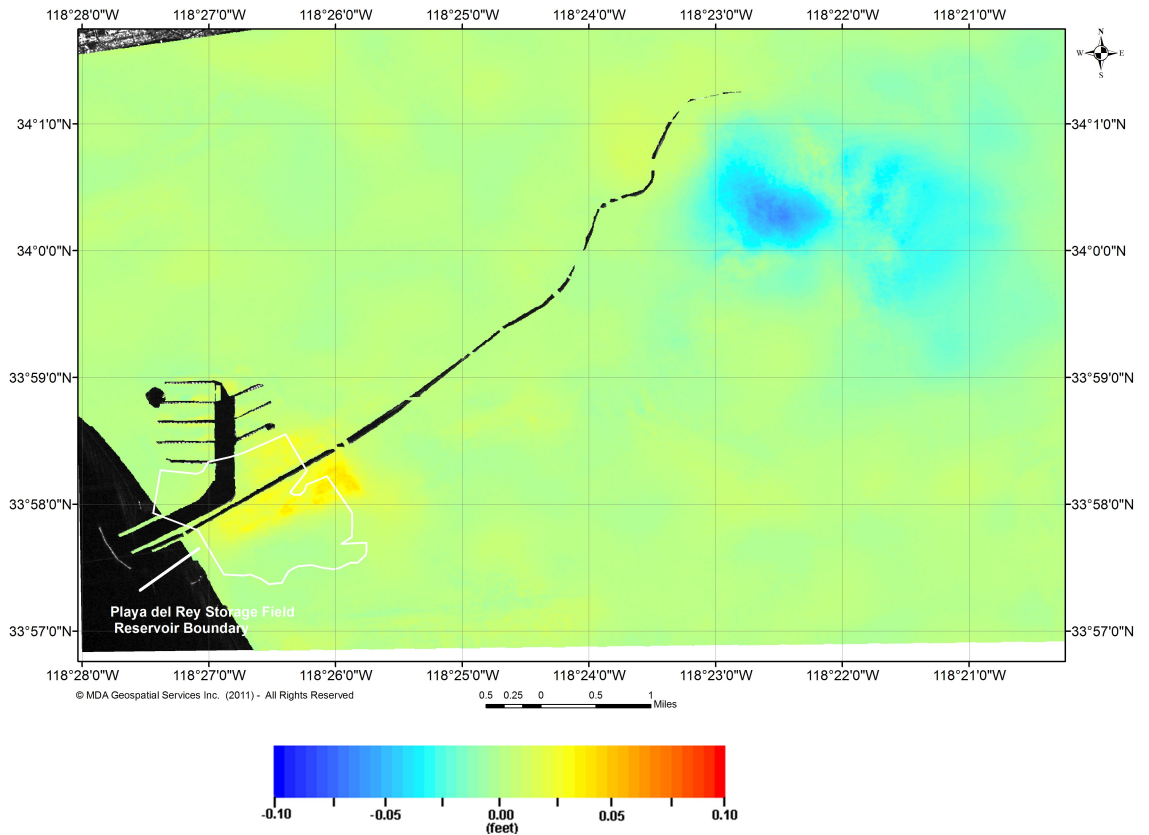


Figure 2: Playa del Rey Gas Storage Field AOI and surrounding area. Color representation of the vertical deformation product from December 19, 2010 to March 1, 2011 superimposed on SAR image without contours. In this representation, blue corresponds to subsidence and red indicates uplift.

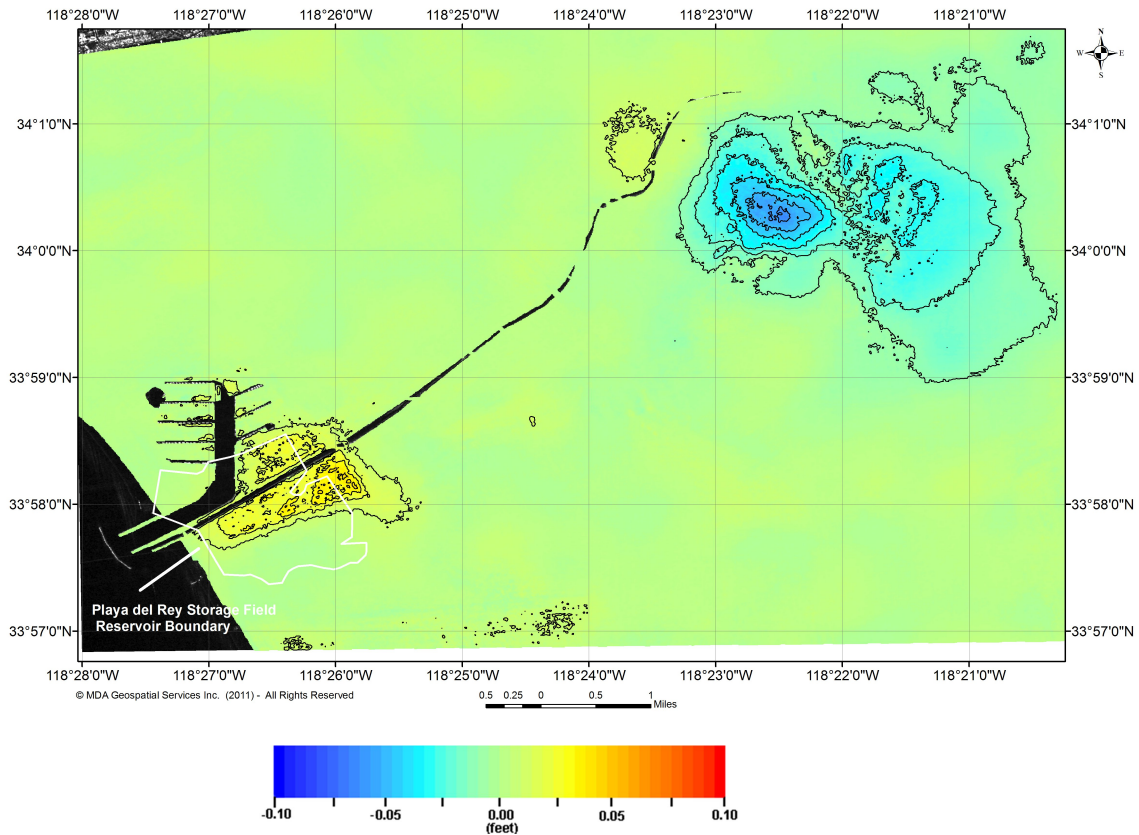


Figure 3: Playa del Rey Gas Storage Field AOI and surrounding area. Color representation of the vertical deformation product from December 19, 2010 to March 1, 2011 superimposed on SAR image with 0.01 ft contours. In this representation, blue corresponds to subsidence and red indicates uplift.

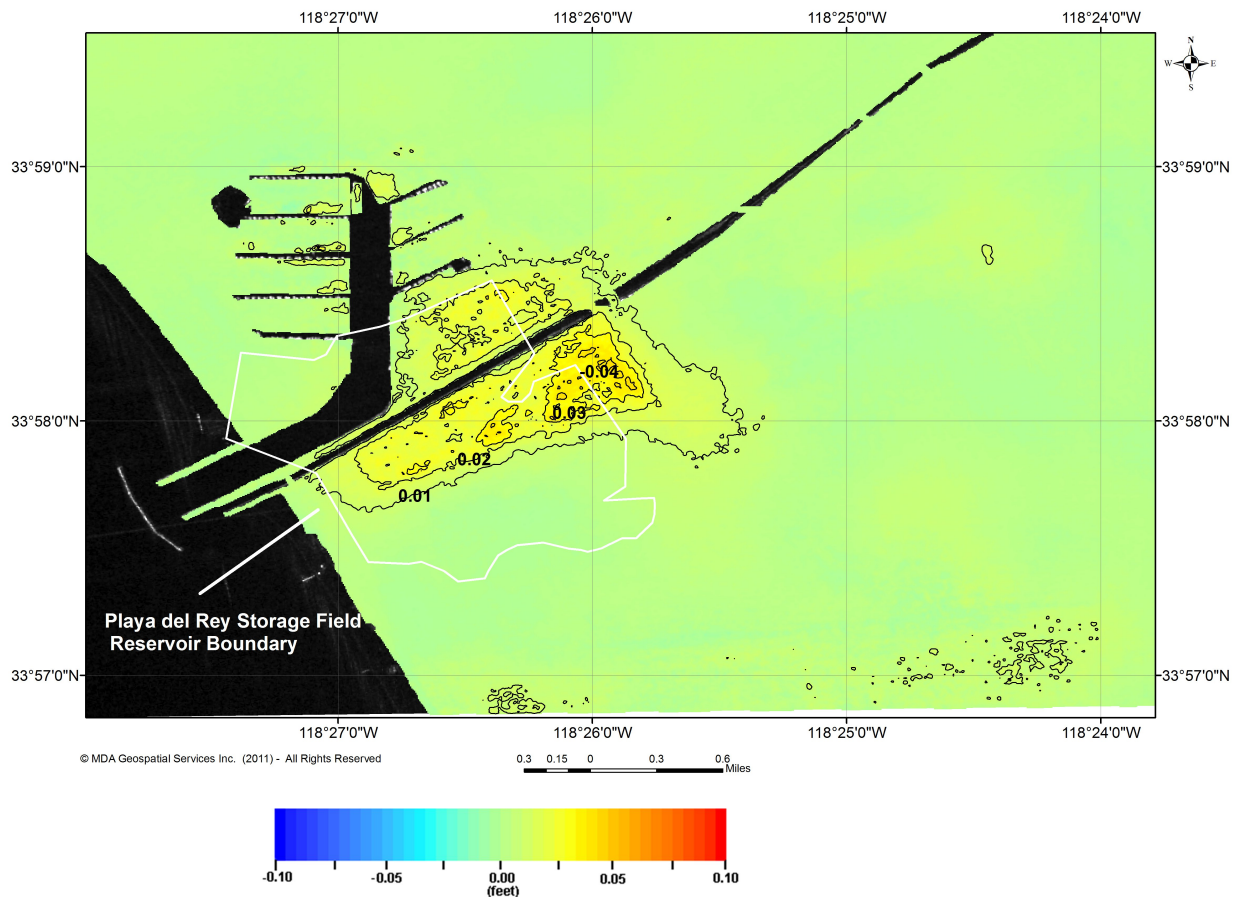


Figure 4: Zoom-in of Playa del Rey Gas Storage Field AOI. Color representation of the vertical deformation product from December 19, 2010 to March 1, 2011 superimposed on SAR image with 0.01 ft contours. In this representation, blue corresponds to subsidence and red indicates uplift.



## **2.2 Pair B - March 1, 2011 to June 29, 2011**

The deformation in the Playa del Rey Gas Storage Field is observed for the time period between March to June 2011, as can be seen from the vertical deformation product shown in Figure 5.

Minimal rainfall occurred during the March to June 2011 time period as recorded by the National Weather Service at LAX (Table 5). Figure 5 show this decrease in natural terrain moisture by the resulting subsidence over the AOI. In the north easterly limits of the Playa del Rey Storage Field Reservoir Boundary, (center coordinate 33°58'17"N 118°25'59"W) deformation values range from 0.03 to 0.04 ft subsidence, as seen in Figure 7.

Figure 6 and Figure 7 present a color representation of the final product. The estimated precision for Pair B is within  $\pm 0.018$  ft with a 95% confidence interval.



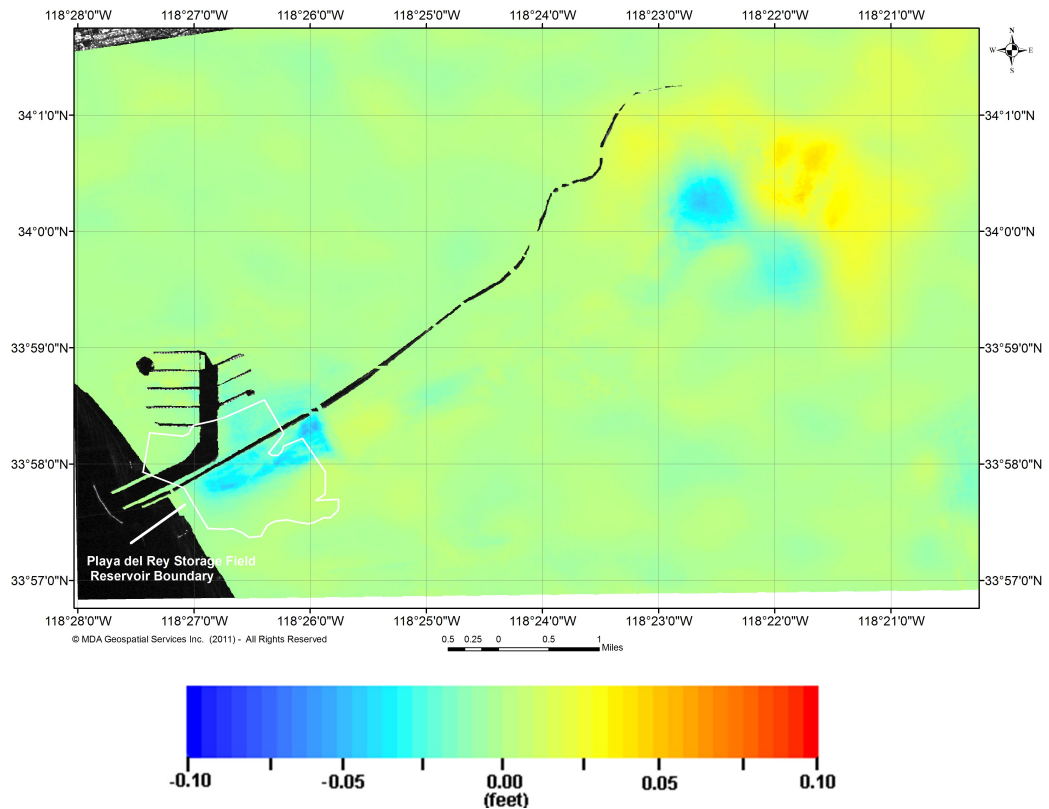


Figure 5: Playa del Rey Gas Storage Field AOI and surrounding area. Color representation of the vertical deformation product from March 1, 2011 to June 29, 2011 superimposed on SAR image without contours. In this representation, blue corresponds to subsidence and red indicates uplift.

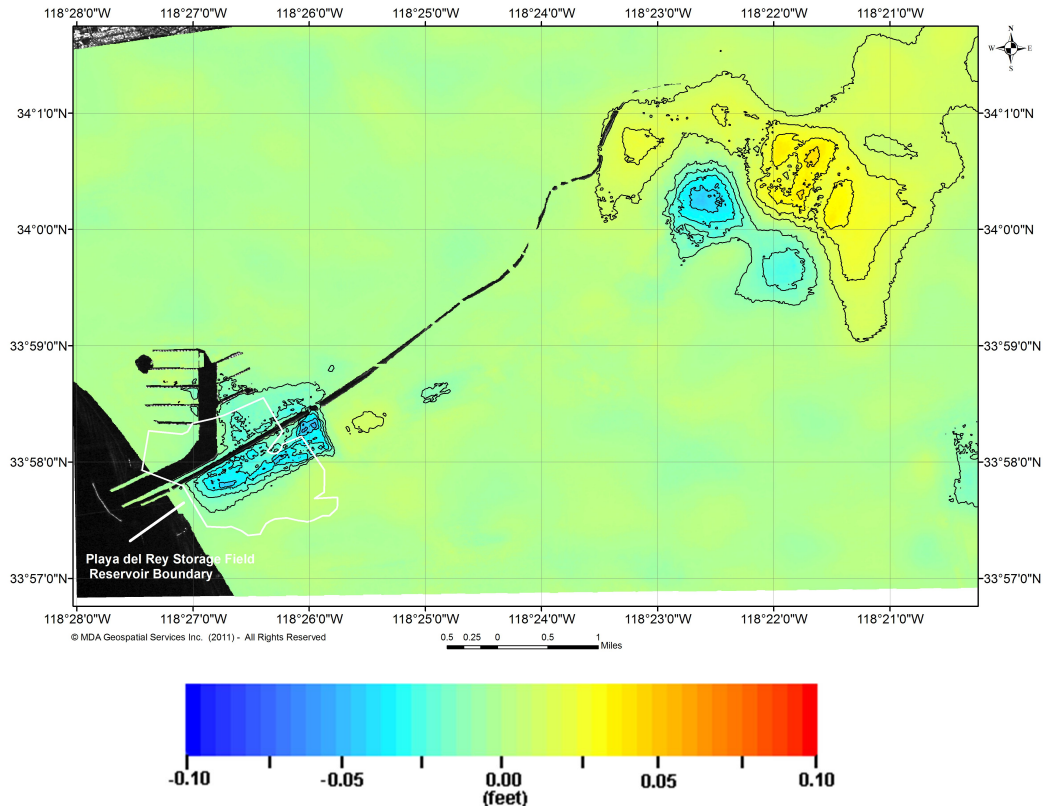


Figure 6: Playa del Rey Gas Storage Field AOI and surrounding area. Color representation of the vertical deformation product from March 1, 2011 to June 29, 2011 superimposed on SAR image with 0.01 ft contours. In this representation, blue corresponds to subsidence and red indicates uplift.

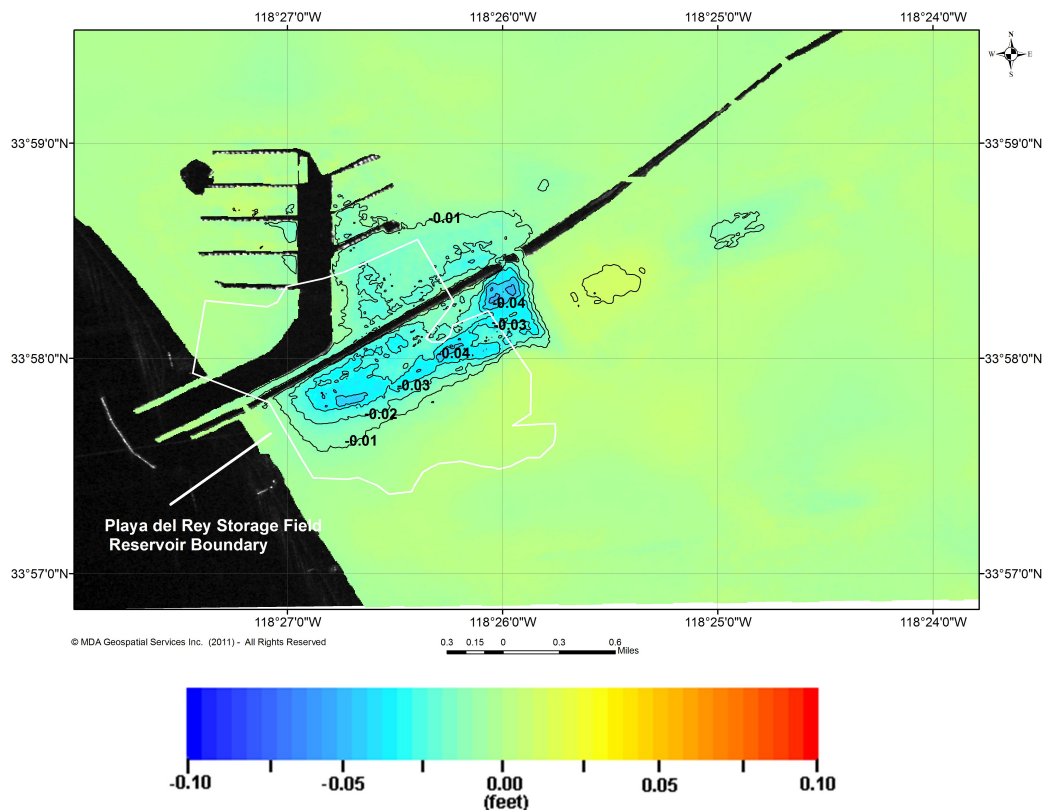


Figure 7: Zoom-in of Playa del Rey Gas Storage Field AOI and surrounding area. Cumulative vertical deformation from March 1, 2011 to June 29, 2011, with 0.01 ft contours.



### **2.3 Pair C - Cumulative Vertical Deformation December 19, 2010 to June 29, 2011**

Pair C represents the cumulative vertically deformation results over the AOI and surrounding areas in Los Angeles from December 2010 to June 2011 (Figure 8).

By enhancing the temporal and spatial accuracy, the use of repeated measurements has reduced the atmospheric noise and highlighted the fact that the actual ground movement in the Playa del Rey Gas Storage Field is negligible (Figure 9).

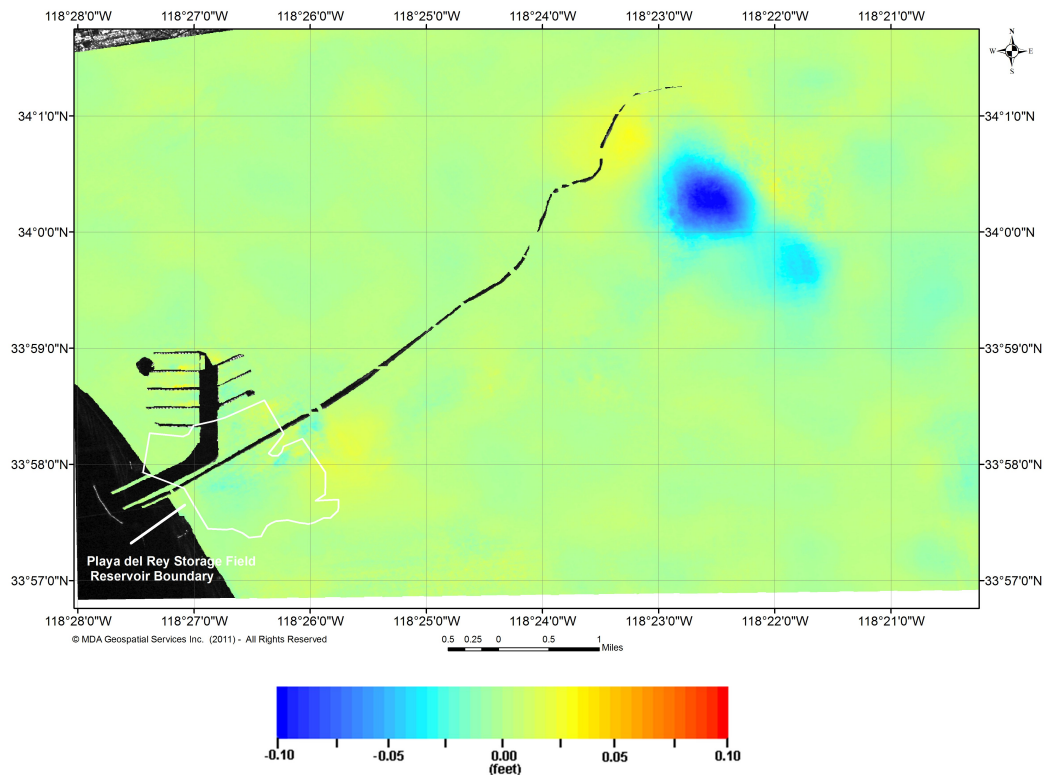


Figure 8: Playa del Rey Gas Storage Field AOI and surrounding area. Color representation of the cumulative vertical deformation from December 19, 2010 to June 29, 2011 superimposed onto SAR image.

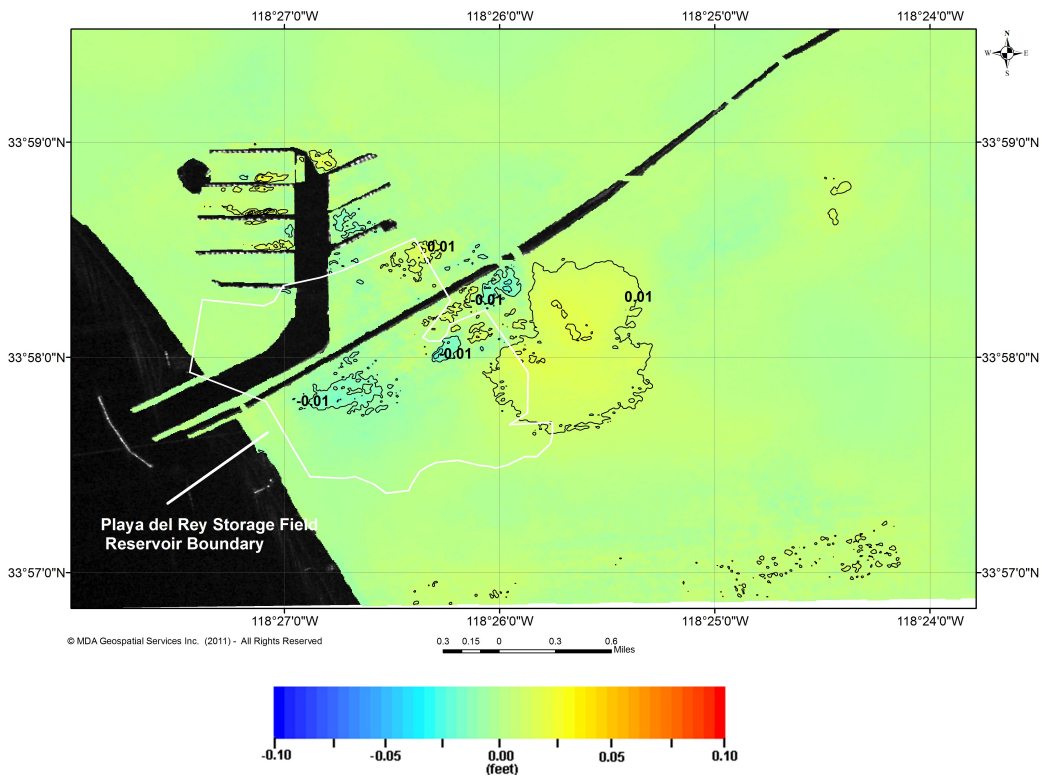


Figure 9: Zoom-in of Playa del Rey Gas Storage Field. Color representation of the summation of the vertical deformation products from December 19, 2010 to June 29, 2011 superimposed on SAR image with 0.01 ft contours. In this representation, blue corresponds to subsidence and red indicates uplift.

## **2.4 Pair D - Cumulative Vertical Deformation May 27, 2008 to June 29, 2011**

Pair D represents the cumulative vertical deformation results over the AOI and surrounding areas in Los Angeles from the start of the monitoring period, May 27, 2008 to the current period analyzed, June 2011 (Figure 11).

Subtle cumulative deformation is observed in the Playa del Rey Gas Storage Field AOI over the 3 year time period. This result is attributed to natural terrain expansion during the time periods when rainfall accumulation is higher than normal.

Subsidence is observed between Ladera Heights and Windsor Hills, center coordinate 33°59' 46"N 118°21' 46"W. Subsidence in this area is in the order of 0.05 - 0.19 ft as shown in Figure 10. Uplift is observed over an area situated between Ladera Heights and Culver City, center coordinate 34°0' 42"N 118°23' 09"W. Uplift in this area is in the order of 0.05 - 0.09 ft.



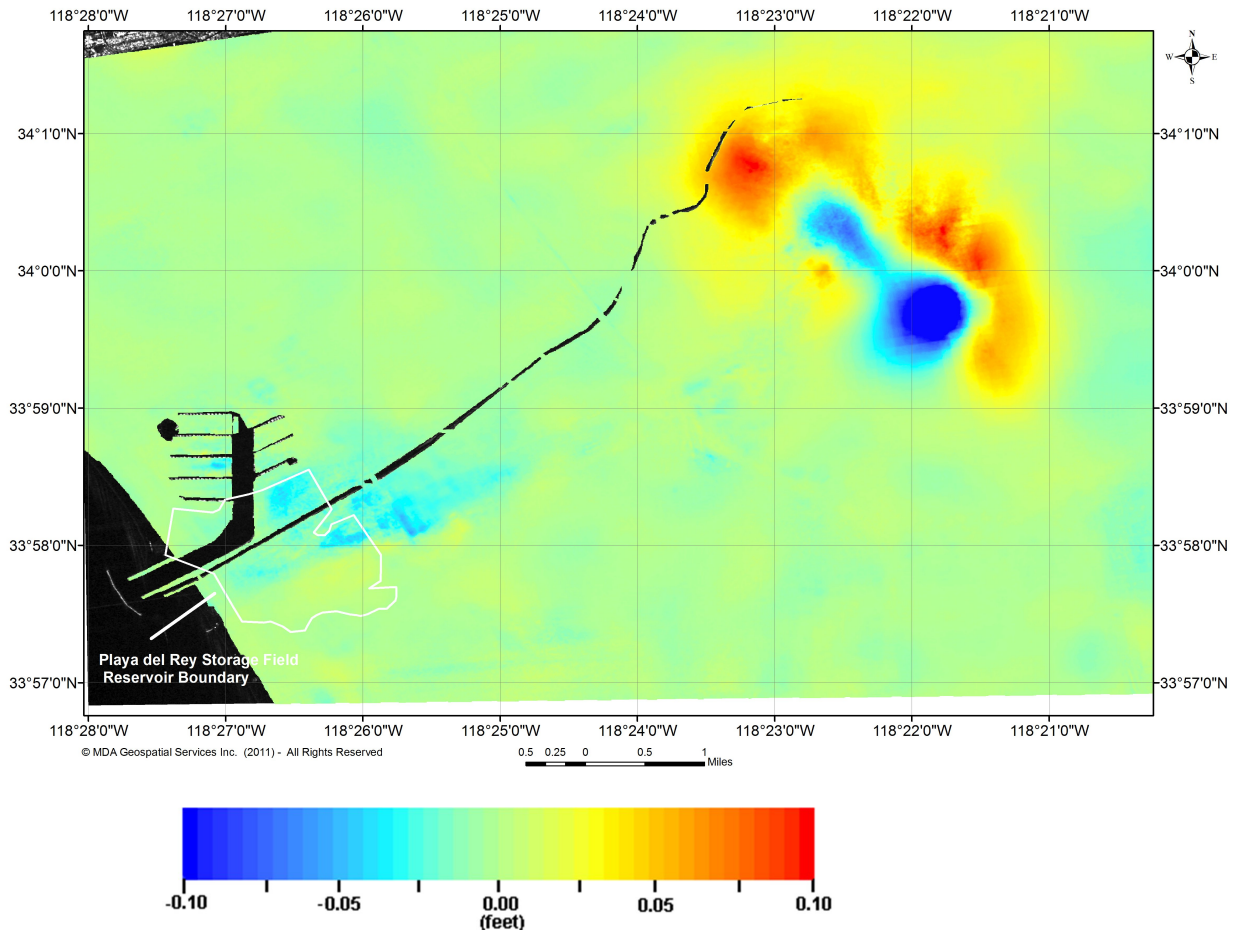


Figure 10: Playa del Rey Gas Storage Field AOI and surrounding area. Color representation of the cumulative vertical deformation from May 27, 2008 to June 29, 2011 superimposed onto SAR image.



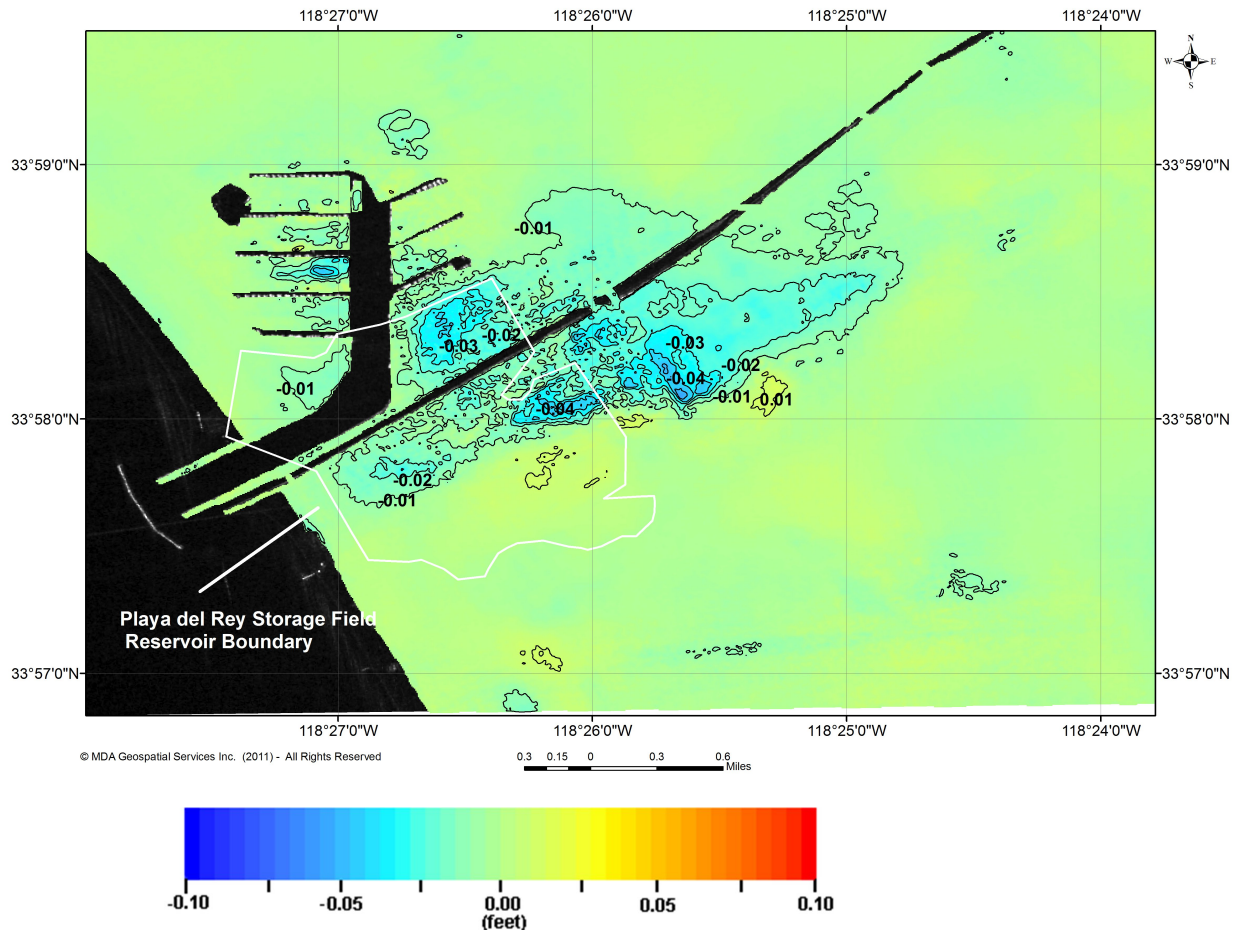


Figure 11: Zoom-in of Playa del Rey Gas Storage Field AOI and surrounding area. Cumulative vertical deformation from May 27, 2008 to June 29, 2011, with 0.01 ft contours.



### 3 Concluding Remarks

Vertical surface deformation measurements are calculated for the Playa del Rey Gas Storage Field and surrounding areas in Los Angeles using conventional InSAR. This report, referred to as Interim Report E, pertains to Milestone 6 of the current contract, RV-14524.

The following items describe the main findings of the work performed, for this milestone:

- RADARSAT-2 Ultra-Fine ascending data were scheduled by MDA for acquisition. The acquired data, covering the period of December 2010 to June 2011, were analyzed and utilized as part of the deliverable.
- Two deformation maps were generated. The estimated precision for the vertical deformation product Pair A, December 19, 2010 to March 1, 2011 is 0.01 ft with a 95% confidence interval. The estimated precision for Pair B, March 1, 2011 to June 29, 2011 is 0.009 ft with a 95% confidence interval.
- For the latest time period analyzed, December 2010 to June 2011, large variations in precipitation have been recorded by the National Weather Service (Table 5). The variation in the reported InSAR ground surface movement is likely related to soil moisture changes. The majority of this variance is within the reported measurement of 0.02 ft, the noise level.
- The resulting analysis from May 2008 to June 2011, indicates that no major deformation is occurring in the Playa del Rey Gas Storage Field.



## A Deliverables

The deliverables, which are included on CD-ROM for Milestone 6, are listed in Table 6. These delivered data are described in XYZ ASCII files and are in California US State Plane, NAD27, 65.62 ft spacing.

Table 6: Delivered Data

<b>Deliverable file</b>	<b>Description</b>
PlayadelRey_SoCalGas_InterimReportE_2011.pdf	Interim Report E in PDF format.
<b>Conventional Deformation map</b>	
121910_030111_DEF.xyz 121910_030111_DEF.tif  030111_062911_DEF.xyz 030111_062911_DEF.tif  SUM_121910_062911_DEF.xyz SUM_121910_062911_DEF.tif  SUM_052708_062911_DEF.xyz SUM_052708_062911_DEF.tif	ASCII files with location and vertical deformation measurements in ft. Areas of low coherence are masked out with values set to -999.  Additional format supplied as Geotiff.
Projection_Report.pdf	Describes the coordinate projection system of the delivered data.



## B Standard Definitions

**Amplitude ( $a$ )** The amplitude of a wave is the distance from the centre of the wave to the peak, see Figure 12.

**Ascending** Satellite tracks that transit from the south to the north are labeled ascending.

**Aspect Angle ( $\alpha$ )** The aspect angle is the angle at which the local area is observed.

**Azimuth** Azimuth or track describes the direction of travel of the sensor over the ground.

**Baseline ( $B$ )** The baseline is the vector describing the distance between two radar observations of the same point (see also perpendicular baseline).

**Coherence ( $\gamma$ )** Coherence,  $\gamma$ , is used as a measure of the degree of similarity between the backscatter (amplitude and phase) response of coregistered SAR returns over time or space.

**Coregistration** Coregistration is the process of locating subsequent radar images to the same observation space. A set of coregistered images show information from the same point on the ground at the same image coordinate.

**Descending** Satellite tracks that transit from the north to the south are labeled descending.

**Electromagnetic Wave** An electromagnetic wave is a self-propagating wave that may exist in a vacuum or in matter. The wave has both electric and magnetic field components that oscillate with perpendicular phase. Electromagnetic radiation exists on a spectrum from gamma-rays to long radio waves. The visible spectrum is narrowly between 400 and 700 nm. Microwaves, the radiation used in SAR observations, are generally between a fraction of a millimetre and a metre in length.

**Frequency ( $f$ )** Frequency describes the number of cycles per second. Frequency is given in Hertz (Hz). For an electromagnetic wave, wavelength,  $\lambda$ , and frequency,  $f$ , are related through the speed of light,  $c$ , as  $c = \lambda f$ .

**Frequency Band** Radar frequencies are often referred to by a band letter. The coding goes back to the research conducted during WWII. C-Band extends from approximately 4-8 GHz. RADARSAT-1 & 2, ENVISAT, and ERS-1 & 2 all operate in C-Band. L-Band at 1-2 GHz was the operating frequency of

the original SEASAT satellite in the 1970s, and the ALOS satellite currently operates in that range. The TerraSAR-X satellite operates in X-Band (8-12 GHz). Figure 13 shows the electromagnetic spectrum.

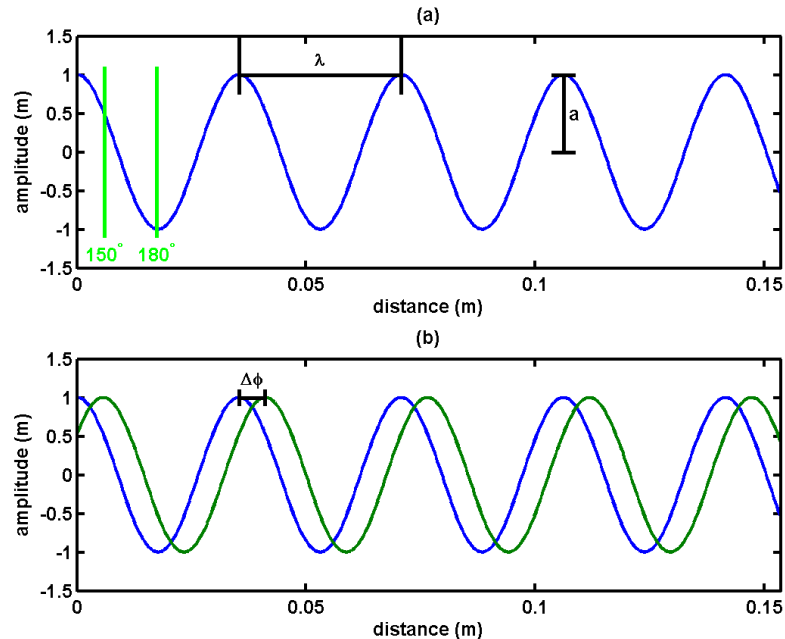


Figure 12: Definition of a 5.6-cm wave. Panel (a) shows the definition of wavelength,  $\lambda$ , and amplitude ( $a$ ). The green lines show the location on the wave associated with  $150^\circ$  and  $180^\circ$  of phase. Panel (b) demonstrates the phase difference,  $\Delta\phi$ , between two waves.

**Georeferencing** Georeferencing is the procedure used to assign individual radar observations to geographic positions. The process involves calculating the geographic position based on the time to target and the observation time of the radar. Georeferencing for RADARSAT-2 has been measured (based only on the state vectors and the imaging geometry) to be better than 20 m on the ground.

**Incident Angle ( $\theta_i$ )** The incident angle is the angle the incident radiation makes with respect to the surface normal. In satellite remote sensing,  $\theta_i$  is often used to describe the angle between the mean surface normal and the incident radiation.

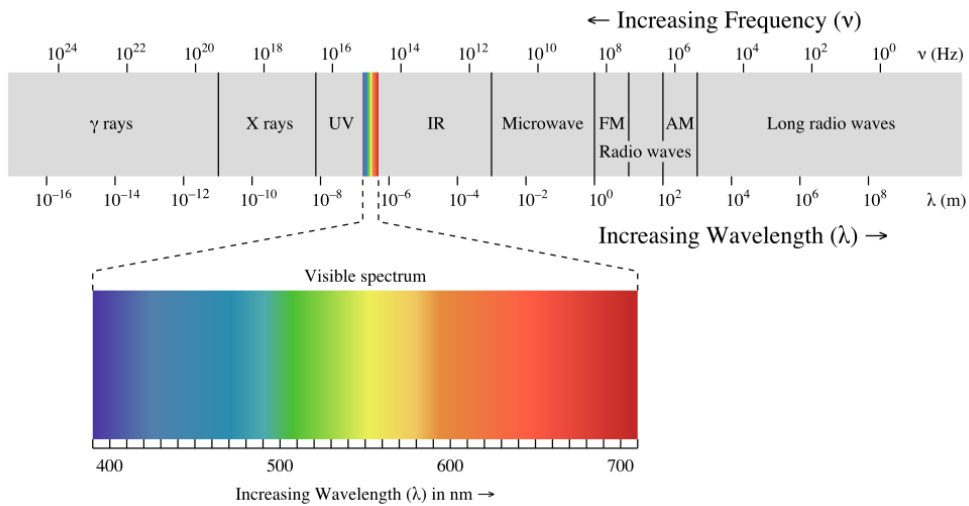


Figure 13: Electromagnetic spectrum showing the wavelength and frequency characteristics of radiation. The microwave portion of the spectrum contains the waves used for RADAR observation.

**Line of Sight** The line of sight describes travel of a wave from the radar to a point on the ground. Observations are only possible along the line of sight.

**Look Direction** Look direction refers to the side of the radar track (or azimuth) that the antenna pattern illuminates. That is, a right looking radar sends energy at approximately  $90^\circ$  to the right of the azimuth track.

**Pass** Pass or pass direction is used to refer to an ascending or descending satellite azimuth.

**Perpendicular Baseline** ( $B_{perp}$  or  $B_{\perp}$ ) is the separation of two radar observations in the direction perpendicular to the first radar observation.

**Phase** ( $\phi$ ) Phase describes the position on a wave. Figure 12 shows a wave with phase labeled as  $150^\circ$  and  $180^\circ$ .  $\phi$  is often reported in radians from 0 to  $2\pi$ , which corresponds to degrees from 0 to 360.

**Phase Difference** ( $\Delta\phi$ ) The phase difference (or phase shift) describes the difference between the position on two waves. Figure 12 shows a phase difference of  $60^\circ$  or  $\pi/3$ . The accuracy with which the phase difference can be measured is why InSAR is so valuable.



**Phase Noise** Phase noise refers to artifacts present in the phase measurement that are not due to the signal we want to capture.

**Range ( $\rho$  or  $R_i$ )** Range is used to describe the distance between a radar target on the ground and the sensor.

**Slant Range** Native SAR observations are recorded by time to target and time of observation. Slant range describes the distance along the radar line of sight.

**Slant Range Coordinates** The coordinate system of the native radar observations, defined by time of observation (azimuth) and time to target (slant range). Observations are aligned as range and azimuth pixels with constant spacing in slant range and slow time.

**Speed of Light ( $c$ )** The speed of light is 299,792,458 m/s.

**Temporal Decorrelation** As the time between observations increases, the physical reasons for the similarity of observations may change. In the monitoring of a field, for instance, the growth of grasses over time will cause decorrelation of the backscatter.

**Wavelength ( $\lambda$ )** Wavelength describes the distance between subsequent points of equal phase in consecutive cycles of a wave.